Journal of Applied Polymer Science

WILEY

Applied Polymer SCIENCE

RESEARCH ARTICLE OPEN ACCESS

From Rigid to Elastic: Tailoring the Properties of Linear Poly(IBOA-co-2EHA) Copolymers Synthesized by UV Polymerization

Djazia Bendeddouche[1] | Lamia Bedjaoui-Alachaher[1] | Aida Jover[2] | Mohammed Aymen Zehouani[1] | Amina Bouriche[1] | Anne-Sophie Schuller[3] | Christelle Delaite[3] | Ulrich Maschke[4]

[1]Laboratoire de Recherche sur les Macromolécules (LRM), Faculté des Sciences, Université Abou bekr Belkaid de Tlemcen, Tlemcen, Algeria | [2]Departamento de Química Física, Facultad de Ciencias, Universidad de Santiago de Compostela, Lugo, Spain | [3]Laboratoire de Photochimie et d'Ingénierie Macromoléculaires (LPIM) EA 4567, Institut de Recherche Jean-Baptiste Donnet, Université de Haute-Alsace, Mulhouse, France | [4]UMR 8207—UMET—Unité Matériaux Et Transformations, Université de Lille, CNRS, INRAE, Centrale Lille, Lille, France

Correspondence: Lamia Bedjaoui-Alachaher (lamia.alachaher@univ-tlemcen.dz) | Ulrich Maschke (ulrich.maschke@univ-lille.fr)

Received: 26 September 2025 | **Revised:** 6 November 2025 | **Accepted:** 7 November 2025

Funding: This work was supported by the Algerian Ministry of Higher Education and Scientific Research (MESRS), the General Directorate of Scientific Research and Technological Development (DGRSDT) of Algeria, University of Tlemcen, Spanish Ministry of Science and Innovation (PID2023-147148NB-I00).

Keywords: crosslinking | glass transition | mechanical properties | photopolymerization | structure-property relationships

ABSTRACT

This study systematically investigated poly(isobornyl acrylate (IBOA)-co-2-ethylhexyl acrylate (2-EHA)) linear random copolymers synthesized via free radical photopolymerization to develop polyacrylate materials with tunable mechanical properties. A series of homopolymers and five copolymer compositions with varying IBOA content were prepared to study the relationship between structure and properties, as well as their correlation with mechanical behavior. The resulting linear polyacrylates were analyzed using multiple techniques. Structural characterization by ^{1}H NMR and MALDI-TOF MS provided detailed information on the chemical environment, molar mass, monomer conversion rate, comonomer sequence distribution within the copolymer backbone, and end-group analysis. Size exclusion chromatography revealed molar mass distributions ranging from 10^5 to 10^6 g/mol. DSC analysis revealed composition-dependent glass transition temperatures and no crystalline melting transitions, confirming the amorphous nature of all copolymers. Tensile testing at room temperature revealed distinct mechanical properties: Poly(IBOA) (PIBOA) exhibited brittle, rigid characteristics, and Poly(2-EHA) (PEHA) displayed flexible, elastic properties. These copolymers demonstrate tunable mechanical properties as a function of comonomer composition, combining the structural rigidity of PIBOA with the flexibility of PEHA. This compositional control over mechanical behavior makes these copolymers promising candidates for applications including biomedical devices, protective coatings, adhesives, and flexible electronics, where tailored mechanical properties are essential.

1 | Introduction

Today's technologies often require the development of new polymer materials tailored for specific applications. Combining two or more monomers to form copolymers is a powerful strategy to enhance physical properties and yield materials with a wide range of characteristics. This versatility makes copolymers highly useful in industries including biomedical devices, drug delivery systems, coatings, and adhesives [1–4].

Homopolymers and copolymers containing an ester group have attracted significant interest due to their versatility in various polymerization reactions, including free-radical and living-radical polymerization [1–4], as well as their applicability in adhesives, biological devices, shape memory polymers, self-healing systems [5–7], drug delivery [8, 9], and 3D/4D printing [10–14].

Polyisobornyl acrylate (PIBOA) has recently gained significant attention due to its unique bicyclic pendant group, which provides stiffness, high chemical resistance, transparency, and a tunable glass transition temperature (T_g). With a T_g well above ambient temperature, PIBOA's properties are comparable to those of poly(methyl methacrylate) (PMMA) and polystyrene, making it suitable for various high-performance applications [15–18]. However, PIBOA can exhibit a high shrinkage rate during photopolymerization [19] and low mechanical resistance below its T_g [20]. Developing PIBOA-based copolymers is therefore an advantageous approach to overcoming these limitations and tailoring properties [21, 22].

Previous research has extensively explored IBOA copolymers. Dong et al. [23] prepared UV-curable waterborne urethane with IBOA to improve water resistance and mechanical properties. Khandelwal et al. [24–26] studied the microstructure of PIBOA homopolymer and IBOA/MMA and IBOA/styrene copolymers using NMR. In our own group's previous work, we have investigated IBOA copolymer systems to achieve specific functionalities: Merah et al. [27] added 2-ethylhexyl acrylate (2-EHA) to IBOA in the presence of 1,6-hexanediol diacrylate to form crosslinked networks with interesting swelling properties; Zeggai et al. [28, 29] developed shape memory polymers based on IBOA and isobutyl acrylate; other work has explored IBOA copolymers with acrylic acid and methacrylic acid for enhanced adhesion to polypropylene surfaces [30]; and Benkhelifa et al. [31] studied the thermal properties of copolymers of IBOA and 2-hydroxy propyl methacrylate.

While these studies established the foundation for modifying IBOA's properties, they primarily focused on crosslinked networks or copolymers with rigid comonomers. In contrast, the specific combination of IBOA with the soft monomer 2-EHA to form well-defined, linear statistical copolymers has not been thoroughly investigated. The novelty of the present work lies in this targeted molecular design and a comprehensive structure–property analysis. We aim to develop a simple, solvent-free UV polymerization method to produce linear statistical copolymers of IBOA and 2-EHA, systematically reducing the material's hardness and tuning its thermomechanical properties. A key aspect of our study is the use of a multi-faceted analytical approach, including MALDI-TOF mass spectrometry for detailed molecular structure determination, to establish clear structure–property relationships in these linear copolymer systems, free from the effects of crosslinking.

2 | Materials and Methods

2.1 | Materials

IBOA (99%) and 2-EHA (99%) were purchased from Sigma-Aldrich and used as received. 2-Hydroxy-2-methyl–1-phenyl propan-1-one (Darocur 1173, Sigma-Aldrich) was used as the photoinitiator.

For matrix-assisted laser desorption/ionization time-of-flight (MALDI-TOF) mass spectrometry analysis, tetrahydrofuran (THF, solvent), trans-2-[3-(4-tert-butylphenyl)-2-methyl-2-propenylidene]malononitrile (DCTB, matrix), and sodium trifluoroacetate (NaTFA, salt) were also supplied by Sigma-Aldrich.

2.2 | Sample Preparation

A series of linear poly(IBOA-co-2EHA) random copolymers with varying IBOA content were synthesized via free-radical photopolymerization. The formulations detailed in Table 1 consisted of IBOA and 2-EHA monomers with 0.5 wt% Darocur 1173 as photoinitiator. Although Darocur 1173 exhibits its primary absorption maximum at a different wavelength, its broad absorption spectrum ensures sufficient sensitivity at 365 nm.

The components were mixed at room temperature for 24 h to achieve homogeneous solutions. Each mixture was then transferred to a disc-shaped Teflon mold with a diameter of approximately 3 cm and a thickness of 0.15 cm, and photopolymerised under a nitrogen atmosphere using a UV chamber equipped with two Philips TL08 fluorescent tubes (λ_(max) = 365 nm, intensity ≈ 0.80 mW/cm^2) for 40 min. The low light intensity was chosen deliberately to moderate the polymerization rate and prevent auto-acceleration effects, thereby promoting more controlled network formation.

A key aspect of this setup is ensuring homogeneous polymerization throughout the sample. The high transparency of the pre-polymerization mixtures at 365 nm ensured efficient light penetration with minimal attenuation. FTIR-ATR spectroscopy confirmed this, showing no significant difference in double bond conversion between the front and back surfaces of the polymerized discs, with conversions reaching ~100% on both sides. This result confirms that a uniform polymer network was achieved without significant gradient effects.

The homopolymers poly(2-ethylhexyl acrylate) and poly(isobornyl acrylate) are designated PEHA and PIBOA, respectively.

TABLE 1 | Formulations used in the UV-induced free-radical polymerization of IBOA and 2-EHA.

	Monomers		Photoinitiator
Designation	IBOA (wt%)	2-EHA (wt%)	Darocur 1173 (wt%)
PIBOA	99.5	0	0.5
Cop 90	89.5	10.0	0.5
Cop 80	79.6	19.9	0.5
Cop 70	69.6	29.9	0.5
Cop 60	59.7	39.8	0.5
Cop 50	49.7	49.8	0.5
PEHA	0	99.5	0.5

Note: The copolymer designation (e.g., Cop 90) indicates the weight percentage of IBOA in the monomer feed. Darocur 1173 was used at a constant concentration of 0.5 wt% relative to the total monomer mass.

The copolymers are labeled Cop 50, Cop 60, Cop 70, Cop 80 and Cop 90, where the number indicates the weight percentage (wt%) of IBOA in the initial feed mixture.

2.3 | Characterization

2.3.1 | Size Exclusion Chromatography

The molar masses (number-average, M_n; weight-average, M_w) and polydispersity ($D = M_w/M_n$) of the synthesized polymers were determined using a Waters Alliance SEC system equipped with a Wyatt refractive index (RI) detector and a Wyatt multi-angle light scattering (MALS) detector (laser wavelength $\lambda = 658$ nm). Separations were performed at 25°C using three Styragel columns (HR1, HR3, and HR4) connected in series. High-performance liquid chromatography (HPLC)-grade tetrahydrofuran (THF) was used as the eluent at a flow rate of 1.0 mL/min. The system was calibrated using narrow dispersity polystyrene (PS) standards from Polymer Laboratories.

2.3.2 | Nuclear Magnetic Resonance Spectroscopy

^{1}H NMR spectra were recorded at 25°C on a Bruker 400 UltraShield spectrometer operating at 400 MHz. The samples were dissolved in deuterated chloroform ($CDCl_3$) containing tetramethylsilane (TMS) as an internal standard. Spectra were acquired with 16 scans.

2.3.3 | Matrix-Assisted Laser Desorption/Ionization Time-Of-Flight Mass Spectrometry

MALDI-TOF mass spectra were acquired in linear positive mode on a Bruker Ultraflex III TOF/TOF mass spectrometer which was equipped with a 337 nm nitrogen laser. The accelerating voltage was 20 kV; the grid voltage and delay time were optimized for each sample to achieve maximum resolution. The laser intensity was maintained just above the threshold to minimize fragmentation, and approximately 250 shots were accumulated per spectrum. The detected mass range was 1–31 kDa.

For analysis, samples were prepared by dissolving the polymer (~10 mg) in THF (1 mL). This solution was then mixed with a matrix solution of *trans*-2-[3-(4-*tert*-butylphenyl)-2-methyl-2-propenylidene]malononitrile (DCTB, 20 mg/mL in THF) and a cationizing agent solution of sodium trifluoroacetate (NaTFA, 10 mg/mL in THF) in a 10:5:1 volume ratio. An aliquot of the final mixture was spotted on the target plate and allowed to dry.

2.3.4 | Differential Scanning Calorimetry

Thermal analysis was performed on a TA Instruments Q2000 DSC under a nitrogen atmosphere. Samples (5–15 mg) were sealed in non-hermetic aluminum pans. The thermal history was erased by a first heating cycle from 25°C to 100°C, followed by cooling to −80°C and a second heating scan to 100°C, all at a rate of 10°C/min. Isothermal holds of 2 min were applied at the end of each heating and cooling segment. The glass transition temperature (T_g) was determined from the midpoint of the transition in the second heating scan. For reproducibility, at least three independently prepared samples of identical composition were analyzed.

2.3.5 | Mechanical Tensile Testing

Quasi-static tensile tests were performed at 22°C using a Mecmesin VersaTest stand equipped with an Advanced Force Gauge (AFG 100 N) transducer. Rectangular specimens ($30 \times 6 \times 1$ mm^3) were gripped using wedge-action clamps and stretched at a constant crosshead displacement rate of 12 mm/min until failure. The Young's modulus was calculated from the initial slope of the stress–strain curve using the tangent modulus method. A minimum of five specimens per composition were tested to ensure reproducibility.

3 | Results and Discussion

As detailed in Table 1 and illustrated in Scheme 1, a series of linear poly(IBOA-co-2EHA) copolymers were synthesized with varying weight fractions of IBOA and 2-EHA.

The SEC elugrams for all compositions are presented in Figure S1. A slight broadening of the molar mass distribution was observed with decreasing 2-EHA content. However, the average molar masses across the copolymer series remained approximately constant, as summarized in Table 2. This consistency indicates that the subsequent analysis of thermal properties is not influenced by variations in molecular weight.

The data for M_n, M_w, and D, for both the copolymers and the PIBOA and PEHA homopolymers are compiled in Table 2. The obtained M_n values for all polymers were sufficiently high to ensure the formation of a physically entangled network. No clear trend in M_n or M_w, was observed with increasing IBOA content, as both parameters remained relatively constant. The dispersities ranged from 1.7 to 2.0, which is consistent with values typical for polymers synthesized by free-radical polymerization. These results align closely with those reported by Zeggai et al. [29] for a similar poly(IBOA-co-isobutyl acrylate) system, where only slight variations in molar mass were noted.

3.1 | NMR Structural Analysis

The chemical structures of both the monomers and the resulting polymers were confirmed by ^{1}H-NMR spectroscopy. Figure 1 presents the spectra of the pure monomers, IBOA and 2-EHA, alongside their respective homopolymers, PIBOA and PEHA. Figure 2 shows the spectra for monomer mixtures and the resulting Cop 50 and Cop 70 copolymers. All spectra were recorded in $CDCl_3$, with residual solvent resonances at

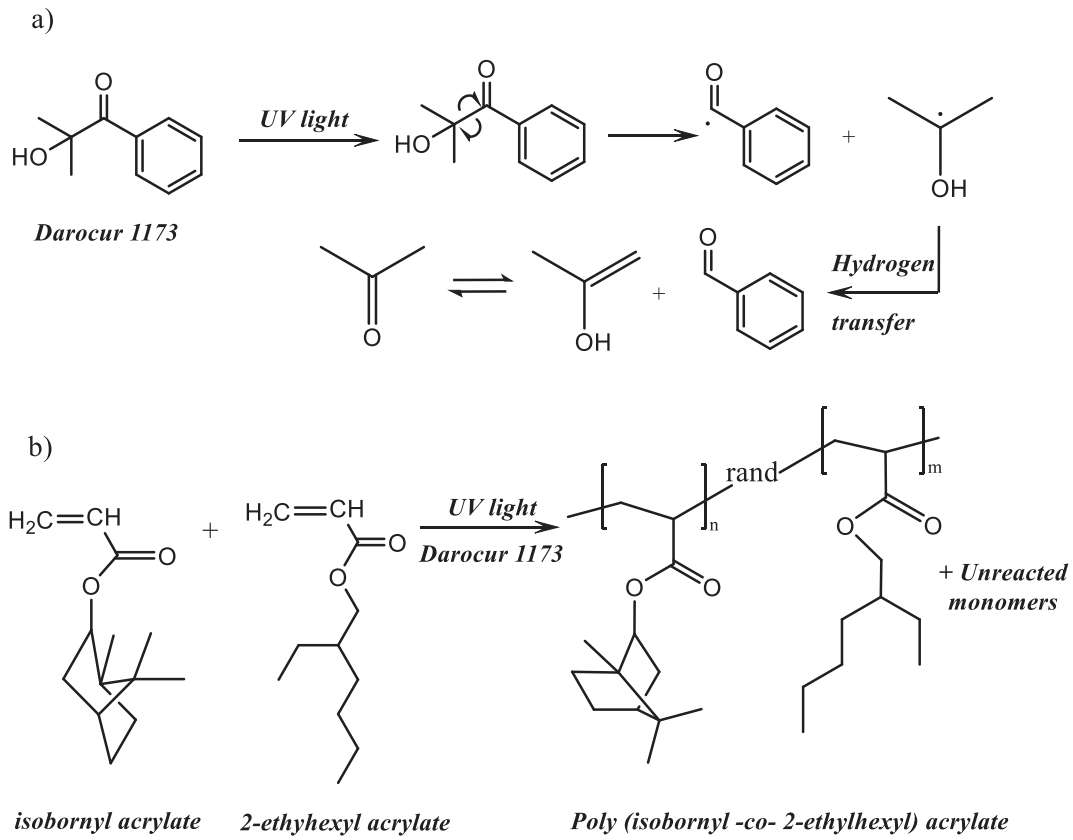

SCHEME 1 | Schematic illustration of the solvent-free UV polymerization process. (a) Initiation step showing the photodissociation of Darocur 1173 to generate free radicals [32]. (b) Propagation step depicting the formation of linear random poly(IBOA-co-2EHA) copolymers from IBOA and 2-EHA monomers.

TABLE 2 | Summary of molar masses and thermal properties for PIBOA, PEHA, and poly(IBOA-co-2EHA) copolymers.

Designation	M_n [10^5 g/mol]	M_w [10^5 g/mol]	D	T_g [°C]
PIBOA	4.7	8.2	1.7	42
Cop 90	5.0	8.5	1.7	41
Cop 80	4.5	8.6	1.9	28
Cop 70	5.5	10.4	1.9	20
Cop 60	5.0	9.6	1.9	−1
Cop 50	4.6	9.3	2.0	−14
PEHA	7.0	11.9	1.7	−66

Note: The copolymer nomenclature (e.g., Cop 50) corresponds to the weight percentage of IBOA in the feed. Values reported are number-average molar mass (M_n), weight-average molar mass (M_w), dispersity ($D = M_w/M_n$), and glass transition temperature (T_g) determined by DSC.

7.28 ppm, acetone at 2.18 ppm, and TMS at 0.09 ppm serving as references.

The complete proton assignments for the monomers and homopolymers are summarized in Table 3 and described below, with proton labels corresponding to the structures in Scheme 1.

3.1.1 | IBOA and PIBOA

In the monomer spectrum, the vinyl protons of the acrylate group (CH_2=CH) resonate between 6.4 and 5.7 ppm. Upon polymerization, these signals disappear, confirming conversion. The characteristic methine proton H_1 (O–CH) of the isobornyl ring appears at 4.77 ppm. The complex signals of the bicyclic ring are observed between 0.87 and 2.0 ppm. Specifically, the methine proton H_3 and axial proton H_{2a} resonate at 1.73–1.77 ppm, while the equatorial proton H_{2e} is found at 1.84 ppm. The equatorial protons H_{4e} and H_{5e} appear at 1.58–1.61 ppm, and their axial counterparts (H_{4a}, H_{5a}) at 1.14–1.20 ppm. The methyl groups are identified at 1.03 ppm (H_6) and 0.87 ppm (H_7, H_8).

3.1.2 | 2-EHA and PEHA

Similarly, the vinyl protons of the 2-EHA monomer (CH_2=CH) are found between 6.4 and 5.7 ppm and vanish after polymerization. The methylene protons H_a (O–CH_2) are observed at 4.09 ppm. The methine proton H_b (>CH) resonates at 1.61 ppm. The aliphatic chain protons (H_c, H_d, H_e) appear as a strong multiplet at 1.29 ppm, while the methylene H_g resonates at 1.39 ppm. The terminal methyl groups H_f and H_h are distinguished at 0.91 and 0.93 ppm, respectively.

The success of the polymerization was confirmed by ^{1}H NMR analysis. Figures 1 and 2 show the disappearance of the vinyl

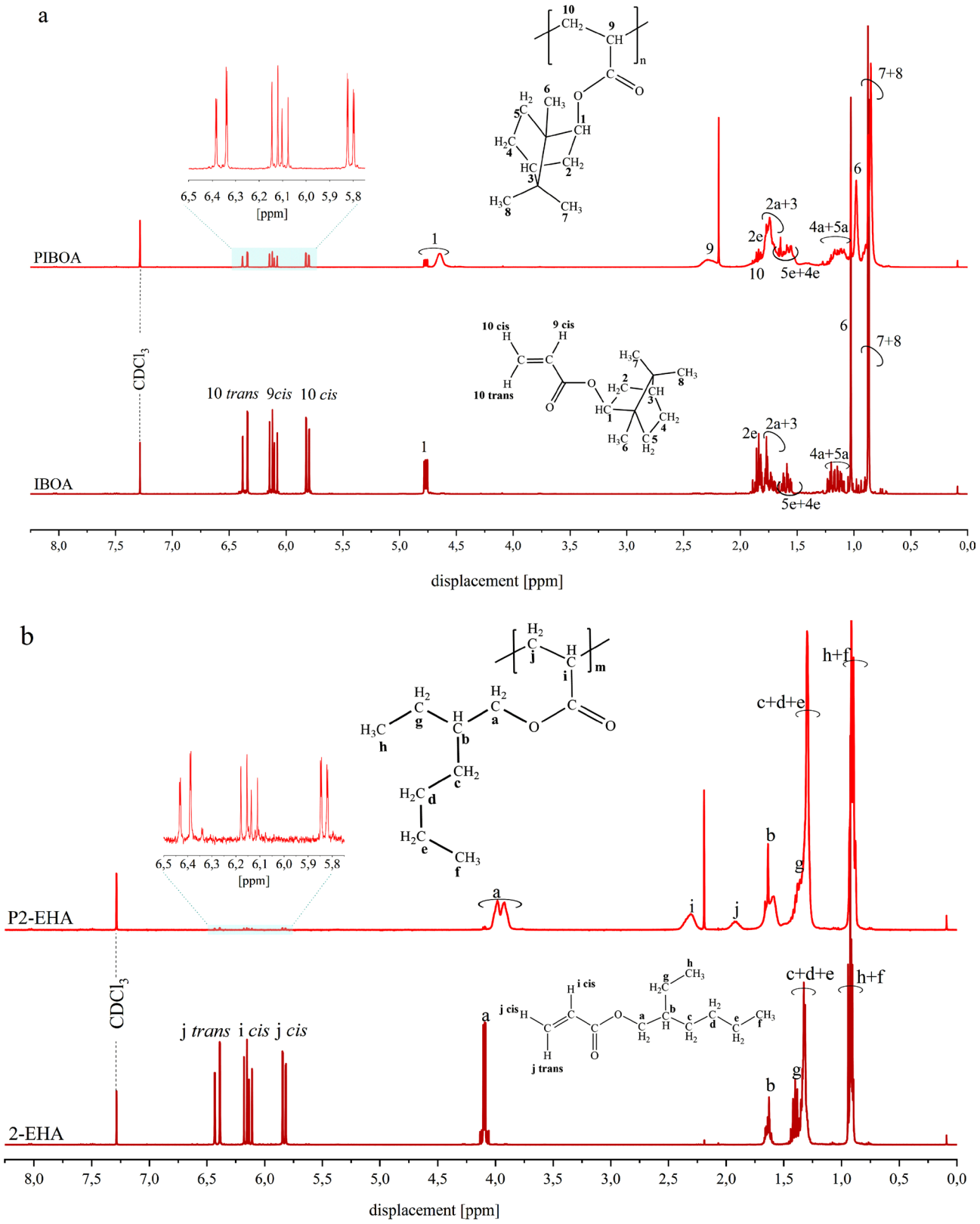

FIGURE 1 | Comparative ^{1}H NMR spectra illustrating the polymerization of (a) IBOA and (b) 2-EHA. For each monomer, the spectrum of the pure monomer is compared to that of its respective homopolymer (PIBOA or PEHA). The key evidence for successful polymerization is the disappearance of the acrylic vinyl proton signals (highlighted region). Proton designations (a: Axial, e: Equatorial) correspond to positions on the isobornyl ring. [Color figure can be viewed at wileyonlinelibrary.com]

proton signals in the region of 5.7–6.4 ppm after the 40-min reaction, indicating consumption of the acrylic double bonds (C═C). Concurrently, new, broad signals appeared in the region of 1.86–2.30 ppm, corresponding to the methine and methylene protons of the polymer backbone (–CH_2–CH–), which confirm the formation of new carbon–carbon (C–C) bonds.

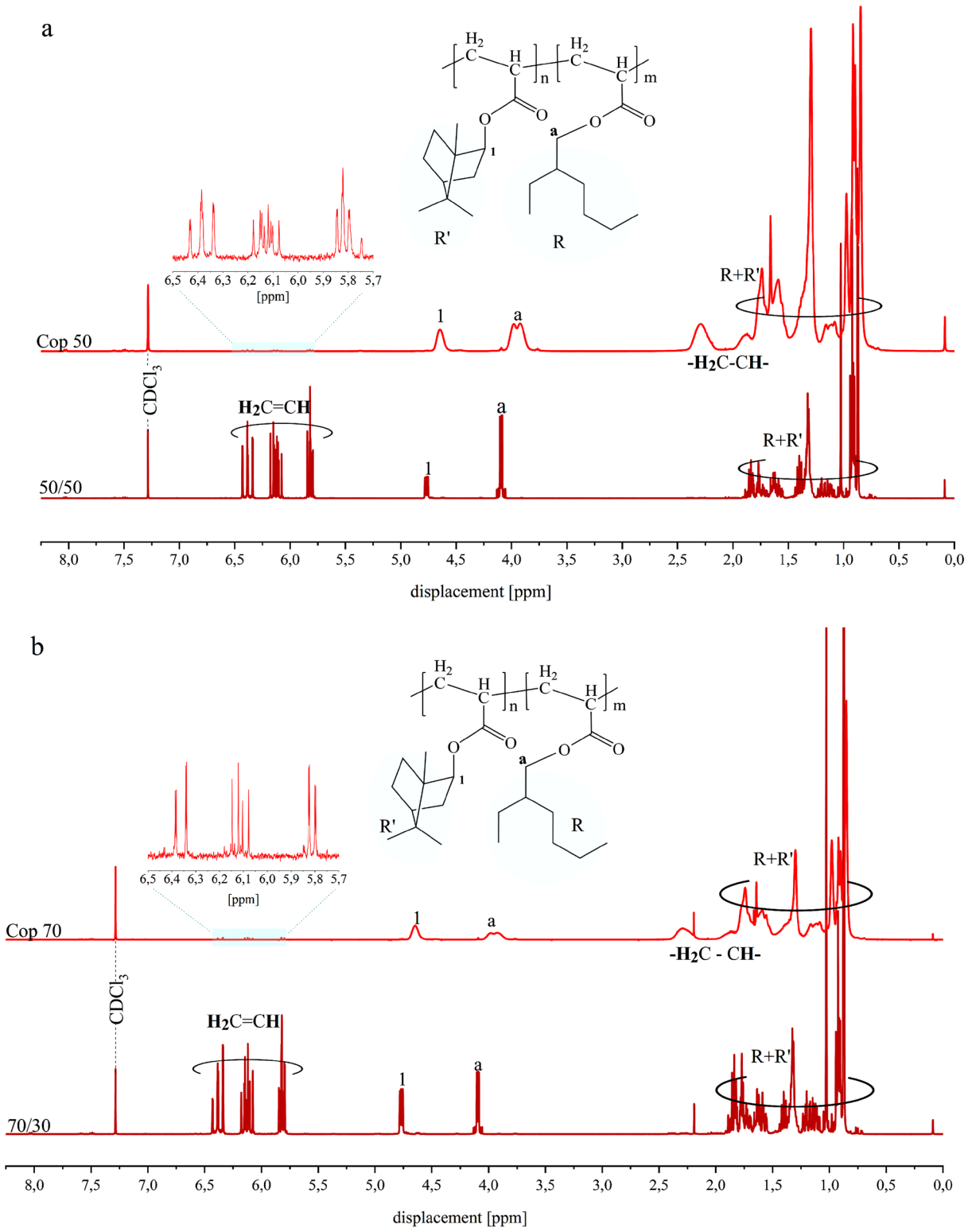

FIGURE 2 | Verification of copolymer formation by ^{1}H NMR. The spectra compare the initial monomer mixtures to the final copolymer products for two compositions: (a) Cop50 (50/50 IBOA/2-EHA feed ratio) and (b) Cop70 (70/30 IBOA/2-EHA feed ratio), recorded in $CDCl_3$ at 25°C. The key evidence for successful polymerization is the consumption of the monomer vinyl bonds (C═C, $\delta = 5.7–6.4$ ppm) and the formation of the polymer backbone (C–C, δ ~1.9–2.3 ppm). The signals from the 2-ethylhexyl (R) and isobornyl (R′) side chains remain present in the copolymers. [Color figure can be viewed at wileyonlinelibrary.com]

Residual vinyl signals indicated incomplete monomer conversion. The molar percentage of unreacted acrylic bonds was calculated using Equations 1 and 2. For PIBOA, the conversion was calculated by comparing the integral of the residual vinyl protons ($H_{9\ cis}$, $H_{10\ cis}$, $H_{\ trans}$) to the integral of the characteristic isobornyl methine proton H_1 (Equation 1). For PEHA, the

TABLE 3 | Assignment of proton chemical shifts for monomers and homopolymers.

Peaks	IBOA	PIBOA	Peaks	2-EHA	PEHA
1	4.79–4.73	4.77–4.64	**a**	4.13–4.04	4.11–3.80
2	**2e**: 1.84	**2e**: 1.84	**b**	1.61	1.63
	2a: 1.77	**2a**: 1.74			
3	1.73	1.77	**c**	1.29	1.30
4	**4e**: 1.58	**4e:** 1.64	**d**	1.29	1.30
	4a: 1.14	**4a:** 1.17			
5	**5e**: 1.61	**5e**: 1.58	**e**	1.29	1.30
	5a: 1.20	**5a**: 1.11			
6	1.03	1.03	**f**	0.91	0.89
7	0.87	0.86	**g**	1.39	1.36
8	0.87	0.86	**h**	0.93	0.92
9cis	6.14–6.07	2.28	**i cis**	6.18–6.10	2.30
10	**cis**: 6.82–6.79	1.86	**j**	**cis**: 5.85–5.80	1.92
	trans: 6.38–6.33			**trans**: 6.44–6.36	

Note: The table lists the ^{1}H NMR resonance frequencies (in ppm) for IBOA, 2-EHA, and their respective homopolymers (PIBOA, PEHA). The proton nomenclature (e.g., 1, 2a/2e for IBOA; a, b for 2-EHA) refers to the atomic positions illustrated in Figure 1. The conversion of vinyl protons (9, 10 in IBOA; i, j in 2-EHA) to aliphatic protons in the polymer backbone is highlighted.

residual vinyl protons ($H_{i\,cis}$, $H_{j\,cis}$, $H_{j\,trans}$) were compared to the methylene protons H_a (Equation 2).

$$\text{PIBOA: \% unreacted acrylic} = \left[I_{(H9cis+H10cis+H10trans)} / \left(I_{H1} \times 3\right)\right] \times 100 \quad (1)$$

$$\text{PEHA: \% unreacted acrylic} = \left[I_{(Hicis+Hjcis+Hjtrans)} / \left(I_{Ha} \times 3/2\right)\right] \times 100 \quad (2)$$

Here, I represent the integral of the specified proton signals. This analysis revealed residual monomer contents of approximately 15% for PIBOA and 2% for PEHA. The copolymers showed higher conversion, with residual acrylic bonds between 2% and 3%.

Furthermore, the copolymer spectra (Figure 2) exhibited the characteristic signals of both comonomers: the methine proton of the IBOA unit (H_1) at ~4.6 ppm and the methylene protons of the 2-EHA unit (H_a) at ~3.9 ppm. The presence of backbone proton signals between 1.9 and 2.3 ppm, along with the comonomer signals, confirms the formation of poly(IBOA-co-2EHA) chains containing sequences of both IBOA and 2-EHA.

The chemical structures of PIBOA, PEHA, and the poly(IBOA-*co*-2EHA) copolymers were further characterized by matrix-assisted laser desorption/ionization time-of-flight (MALDI-TOF) mass spectrometry. This technique provides detailed information on repeat units, end groups, and minor species within a polymer sample [33–37].

MALDI-TOF mass spectra acquired in reflectron mode for PIBOA, PEHA, Cop 50, and Cop 70 showed well-resolved peaks in the m/z range of 1000–6000, enabling reliable assignment to corresponding $(IBOA)_n$ and $(2\text{-}EHA)_m$ oligomeric sequences. Representative segments of the spectra for PIBOA, PEHA, Cop 50, and Cop 70 are presented in Figures 3–6, respectively. The spectra for Cop 60, Cop 80, and Cop 90 are provided in the Figure S2.

It is important to note that the detected oligomers (up to ~3000 g/mol) represent a low molar mass fraction of the sample. This is a common observation in MALDI-TOF analysis of high polymers, as the technique can favor the ionization and detection of lower mass chains. The weight-average molar mass (M_w) of approximately 1,000,000 g/mol determined by SEC is more representative of the bulk material. A similar discrepancy has been reported in other studies of high-molar-mass acrylic copolymers [38].

A detailed analysis of the PIBOA spectrum (Figure 3) reveals a regular mass interval of 208 Da between major peaks, corresponding to the molar mass of the IBOA repeating unit ($C_{13}H_{20}O_2$). For instance, the peak at $m/z = 1792.83$ can be assigned to an octamer (8 IBOA repeat units) initiated by a benzoyl radical (from the Darocur 1173 photoinitiator) and terminated with a hydrogen atom, ionized by a single sodium adduct ($[(C_{13}H_{20}O_2)_8 + C_6H_5CO + H + Na]^+$).

Similarly, the MALDI-TOF spectrum of PEHA (Figure 4) exhibits a regular mass interval of 184 Da, corresponding to the molar mass of the 2-EHA repeating unit ($C_{11}H_{20}O_2$). Assuming an identical end-group structure (benzoyl initiator, hydrogen terminator, and a single sodium adduct), the peak at $m/z = 1968.23$ is assigned to a decamer comprising ten 2-EHA repeat units.

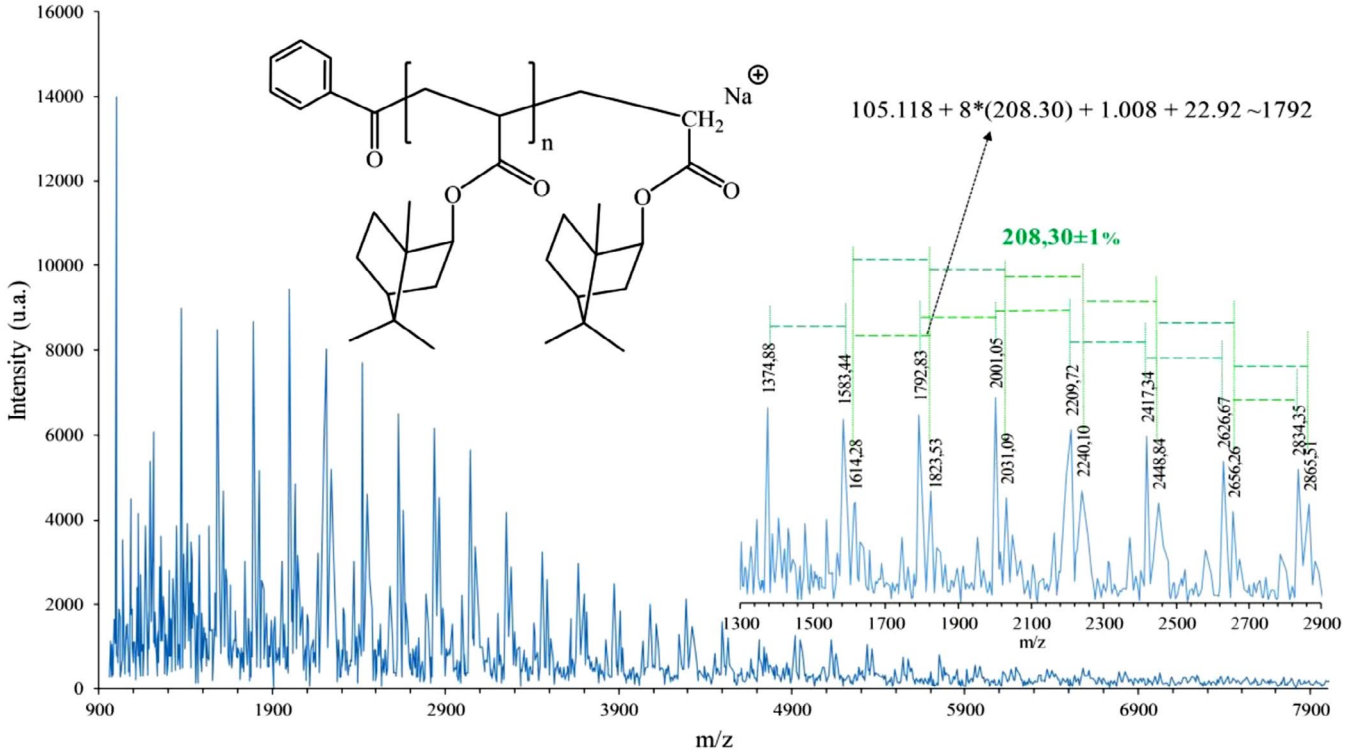

FIGURE 3 | MALDI-TOF mass spectrum of PIBOA. The spectrum shows a series of peaks corresponding to hydrogen-terminated oligomers containing n repeats of the IBOA unit ($C_{13}H_{20}O_2$, 208 Da), initiated by a benzoyl fragment (from Darocur 1173) and ionized by a single sodium cation. The regular mass difference of 208 Da between consecutive peaks (exemplified by the assignment for the octamer, $m/z = 1792.83$) confirms the PIBOA structure. [Color figure can be viewed at wileyonlinelibrary.com]

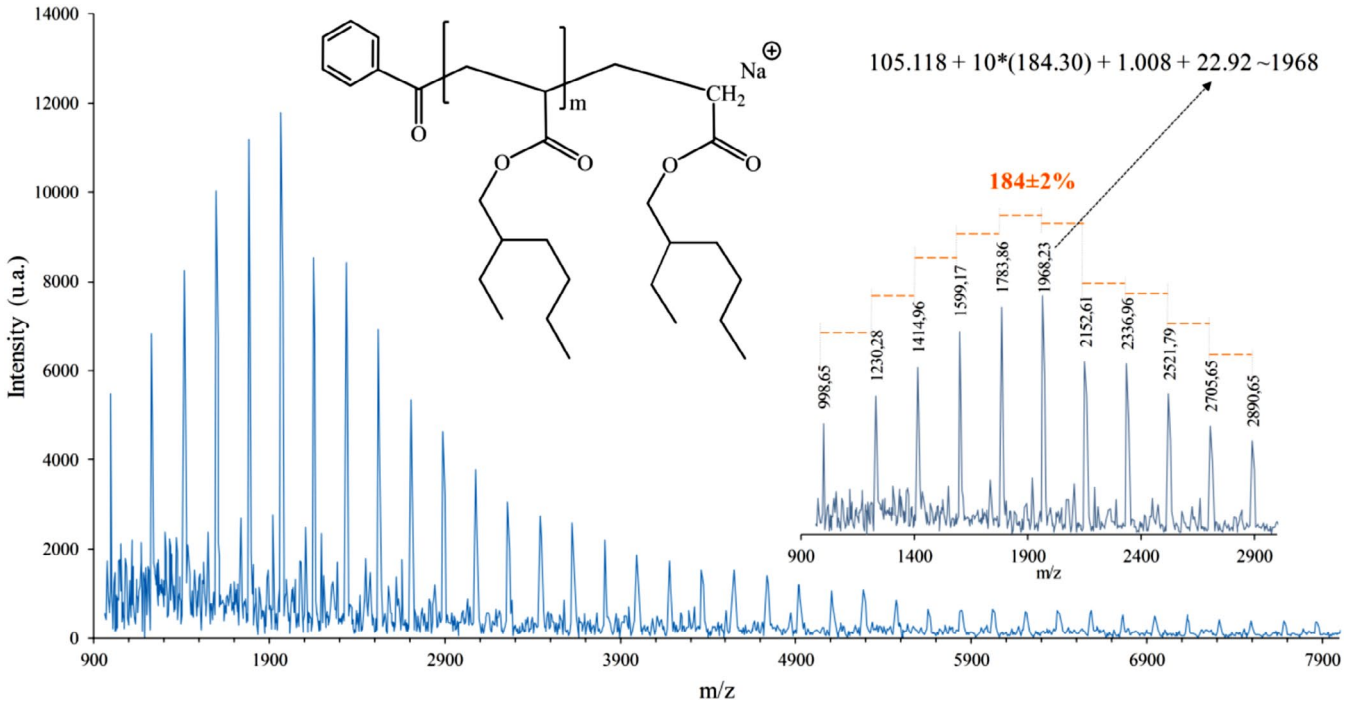

FIGURE 4 | MALDI-TOF mass spectrum of PEHA. The spectrum displays a series of peaks assigned to hydrogen-terminated oligomers containing n repeats of the 2-EHA unit ($C_{11}H_{20}O_2$, 184 Da), initiated by a benzoyl fragment and ionized by a single sodium cation. The consistent mass difference of 184 Da between peaks (as illustrated by the decamer at $m/z = 1968.23$) confirms the PEHA structure and the proposed end-group configuration. [Color figure can be viewed at wileyonlinelibrary.com]

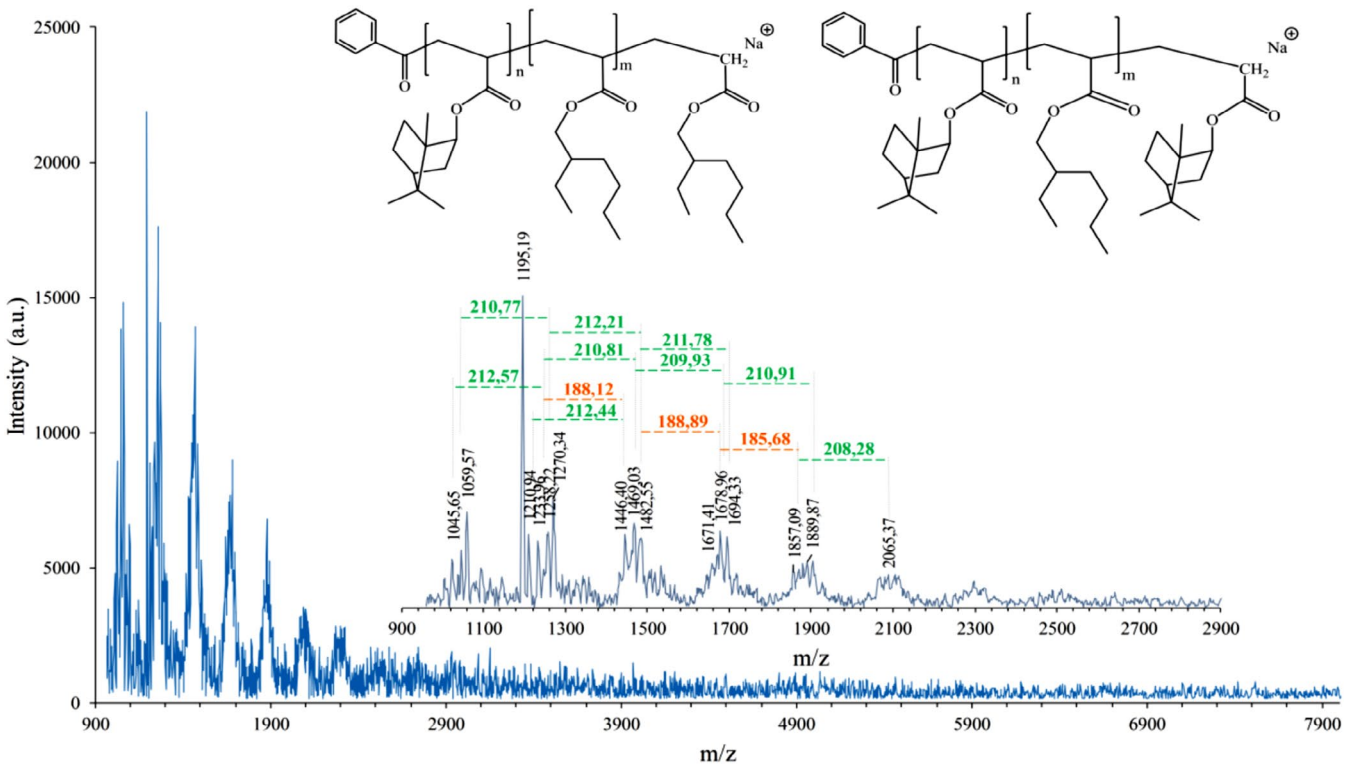

FIGURE 5 | MALDI-TOF mass spectrum of the Cop 50 copolymer (50/50 IBOA/2-EHA feed ratio). The complex peak pattern corresponds to a mixture of co-oligomers containing varying sequences of IBOA (208 Da) and 2-EHA (184 Da) repeat units. The peak at $m/z = 1857.09$, for example, is assigned to an oligomer with a benzoyl initiator and hydrogen terminator containing 3 IBOA ($n = 3$) and 6 2-EHA ($m = 6$) units, ionized by a single sodium cation ($[M + Na]^+$). [Color figure can be viewed at wileyonlinelibrary.com]

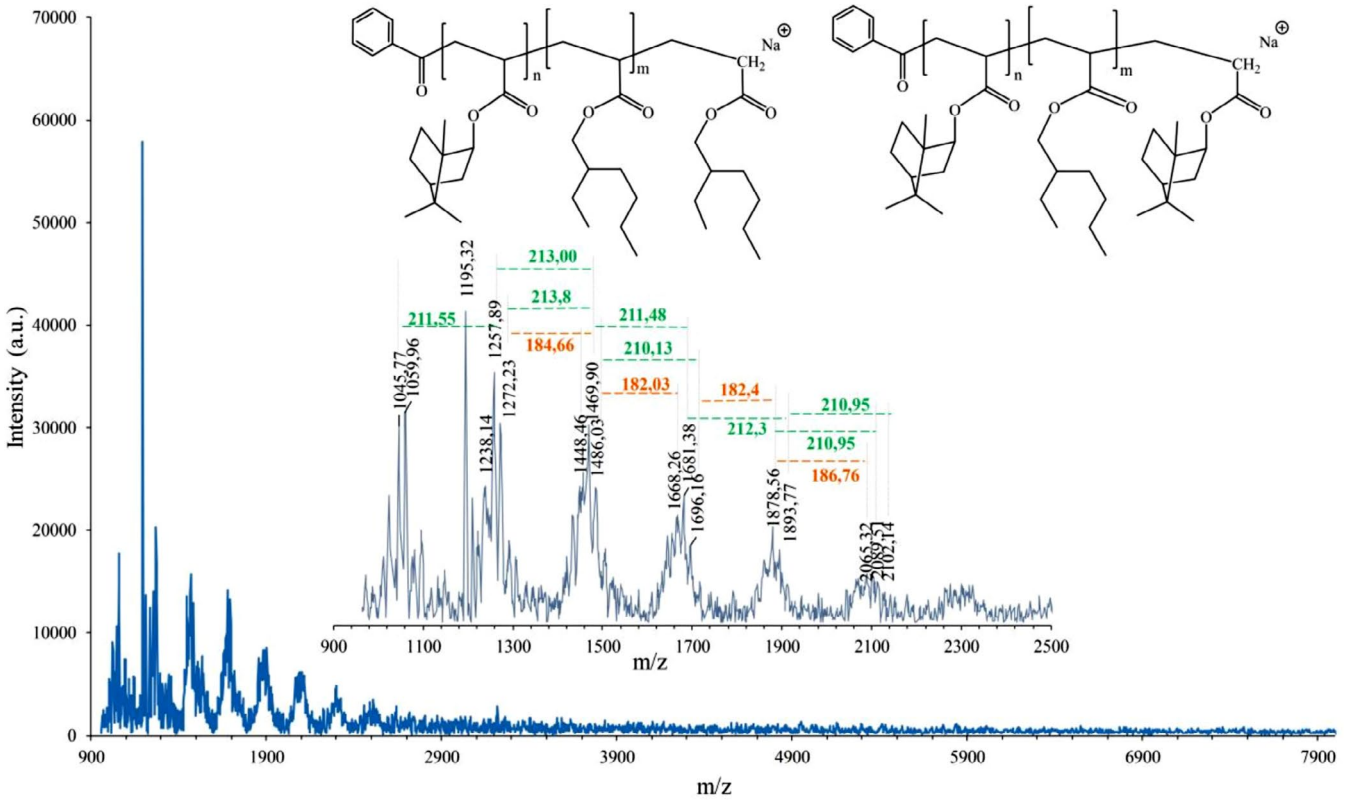

FIGURE 6 | MALDI-TOF mass spectrum of the Cop 70 copolymer (70/30 IBOA/2-EHA feed ratio). The spectrum shows a distribution of co-oligomers incorporating both IBOA (208 Da) and 2-EHA (184 Da) repeat units. The exemplary peak at $m/z = 1469.90$ is assigned to a sodiated oligomer ($[M + Na]^+$), initiated by a benzoyl group and terminated with hydrogen, comprising 2 IBOA ($n = 2$) and 5 2-EHA ($m = 5$) units. [Color figure can be viewed at wileyonlinelibrary.com]

The spectra of the copolymers, Cop 50 and Cop 70 (Figures 5 and 6, respectively), show mass intervals indicative of co-oligomers containing both IBOA (208 Da) and 2-EHA (184 Da) repeating units. For Cop 50, the peak at $m/z = 1857.09$ is consistent with an oligomer containing 3 IBOA ($n = 3$) and 6 2-EHA ($m = 6$) units. For Cop 70, the peak at $m/z = 1469.90$ corresponds to an oligomer with 2 IBOA ($n = 2$) and 5 2-EHA ($m = 5$) units. In both cases, the proposed structures feature a benzoyl initiator, a hydrogen terminator, and are ionized by a single sodium cation.

To comprehensively assign the copolymer spectra, a Python program was developed to calculate the theoretical m/z values for all possible combinations of IBOA (n) and 2-EHA (m) repeat units, considering the specified end groups and sodium adduct. Table 4 displays a selection of the calculated values that match the experimental data with a mass error (Δ) of ±4 Da. The complete calculation results for Cop 60, Cop 80, and Cop 90 are provided in the Table S1.

The thermal properties of the homopolymers and copolymers were analyzed using DSC from −80°C to 100°C. The resulting thermograms are shown in Figure 7, and the corresponding glass transition temperatures (T_g) are summarized in Table 2.

A single, composition-dependent T_g was observed for each copolymer, with values ranging from −66°C (T_g of PEHA) to 42°C (T_g of PIBOA). The presence of a single T_g intermediate between those of the homopolymers is characteristic of a random distribution of comonomer units along the polymer chain. This finding is consistent with the structural information obtained from MALDI-TOF MS.

The T_g decreased systematically with increasing 2-EHA content. This trend is attributed to the flexible, long pendant group of the 2-EHA unit, which increases chain mobility and free volume. In contrast, the rigid, bulky isobornyl group of the IBOA unit acts as a hard segment, restricting chain motion and increasing the T_g.

Although the T_g of various IBOA-based copolymers have been documented in earlier studies [27–29, 31], this work provides—to the best of our knowledge—the first reported T_g values for linear random copolymers of IBOA and 2-EHA. The results establish a clear structure–property relationship for this specific copolymer system. Notably, the T_g values observed here for linear copolymers differ from those reported for compositions of similar monomer content but incorporating minor amounts of diacrylate crosslinker, as described in our previous publication [27]. This divergence underscores the considerable influence of network formation on chain mobility and resultant thermal properties.

The mechanical performance of the copolymers was evaluated through tensile testing at 22°C. Figure 8 shows the resulting stress–strain curves for Cop 80, Cop 70, Cop 60, and Cop 50, from which key parameters—including yield strength, Young's modulus, stress and elongation at break, and toughness—were determined to assess their mechanical performance [39, 40]. These parameters are compiled in Table 5 and reveal a remarkable transition from rigid to highly elastic materials that is directly tunable by the IBOA/2-EHA composition, establishing a clear structure–property relationship essential for material design.

TABLE 4 | Structural assignment of co-oligomers from Cop 50 and Cop 70 based on MALDI-TOF MS analysis.

	Peak positions		IBOA	2-EHA	Δ
Compositions	m/z_{exp}	m/z_{calc}	n	m	$m/z_{exp} - m/z_{calc}$
Cop 50	1233.96	1234.74	0	6	−0.78
	1258.22	1258.77	1	5	−0.55
	1446.40	1443.04	1	6	+3.36
	1469.03	1467.07	2	5	+1.96
	1671.41	1675.37	3	5	−3.96
	1678.96	1675.37	3	5	+3.59
	1857.09	1859.64	3	6	−2.55
	2065.37	2067.94	4	6	−2.57
Cop 70	1238.14	1241.54	0	6	−3.40
	1257.89	1257.01	1	5	+0.88
	1469.90	1472.73	2	5	−2.83
	1696.16	1692.92	4	4	+3.24
	2065.32	2062.70	4	6	+2.62
	2089.51	2087.05	5	5	+2.46

Note: The table lists the experimental mass-to-charge ratios (m/z_{exp}), the corresponding calculated values (m/z_{calc}), and the proposed number of IBOA (n) and 2-EHA (m) repeating units for each assigned peak. All structures are consistent with benzoyl-initiated and hydrogen-terminated chains ionized as single sodium adducts. The mass discrepancy ($\Delta = m/z_{exp} - m/z_{calc}$) is provided for each entry.

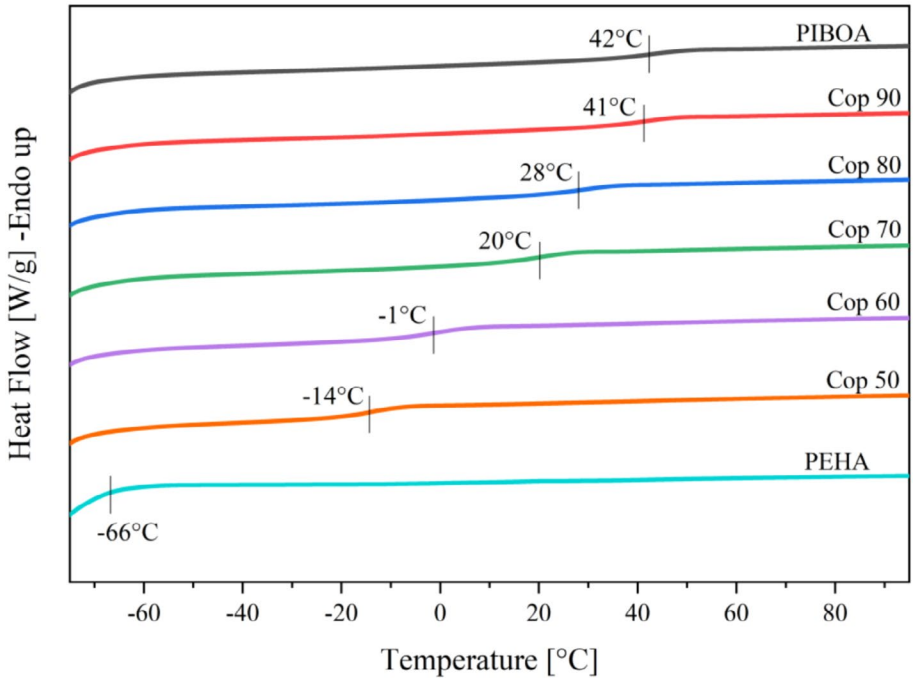

FIGURE 7 | DSC thermograms (second heating scan) of PIBOA, PEHA, and the poly(IBOA-co-2EHA) copolymers. Each copolymer exhibits a single, composition-dependent T_g between those of the homopolymers, indicating the formation of random copolymers. The T_g values are reported in Table 2. [Color figure can be viewed at wileyonlinelibrary.com]

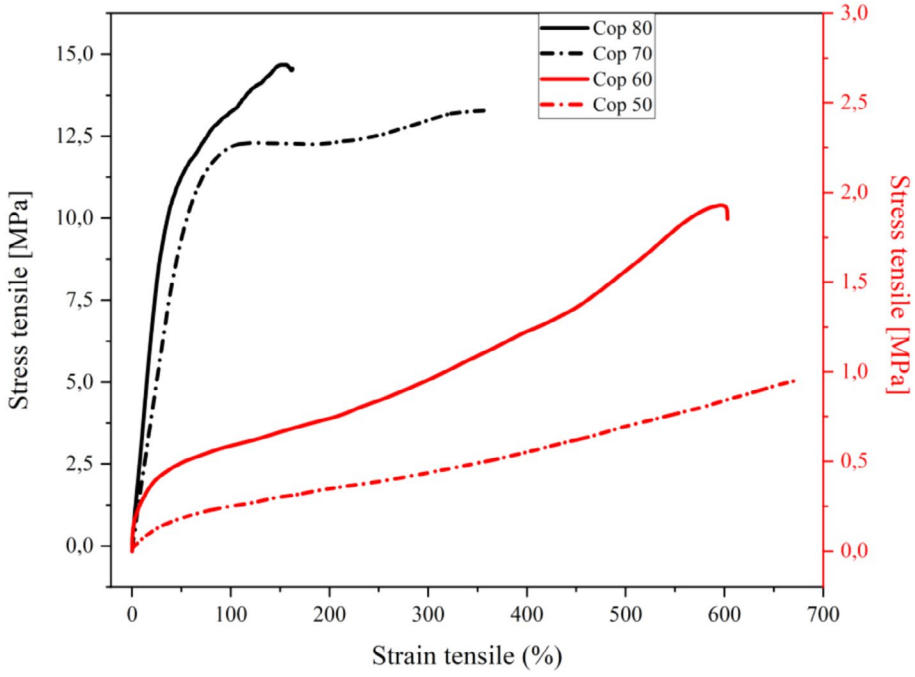

FIGURE 8 | Engineering stress–strain curves from tensile testing at 22°C for the poly(IBOA-co-2EHA) copolymers. The curves demonstrate the transition from rigid, brittle behavior (Cop 80) to soft, elastomeric behavior (Cop 50) as the content of the flexible 2-EHA comonomer increases. Key mechanical parameters derived from these curves are summarized in Table 5. [Color figure can be viewed at wileyonlinelibrary.com]

Copolymers with high IBOA content, such as Cop 80, exhibit behavior characteristic of a rigid plastic. With a T_g significantly above the test temperature of 22°C, it displays a high Young's modulus of 0.316 MPa and a high yield strength of 12.4 MPa, but limited elongation of just 162.3%. It fractures in a brittle manner, without any distinct plastic deformation zone.

In contrast, as the 2-EHA content increases through Cop 70, Cop 60, and Cop 50, the T_g drops below the test temperature, leading to a dramatic shift toward elastomeric behavior. These materials exhibit progressively lower modulus and yield strength, coupled with vastly improved elongation at break, exceeding 600% for Cop 50 and Cop 60. This transition is attributed to the flexible

TABLE 5 | Summary of mechanical properties for the poly(IBOA-co-2EHA) copolymers.

	Tensile test results				
Composition	**Yield strength [MPa]**	**Young's modulus [MPa]**	**Stress at break [MPa]**	**Elongation at break (%)**	**Toughness [MJ/m³]**
Cop 80	12.4 ± 0.042	0.316 ± 6 0.10^{-4}	14.53 ± 17 0.10^{-4}	162.3 ± 0.2	1857.8 ± 8.6
Cop 70	11.7 ± 0.065	0.204 ± 1 0.10^{-4}	13.30 ± 5 0.10^{-4}	361.4 ± 0.2	4106.8 ± 7.2
Cop 60	0.3 ± 0.008	0.169 ± 1.3 0.10^{-6}	1.90 ± 1.18 0.10^{-6}	602.5 ± 0.3	626.6 ± 14.4
Cop 50	0.2 ± 0.001	0.005 ± 0.1 0.10^{-4}	0.95 ± 5 0.10^{-4}	673.4 ± 0.2	340.6 ± 3.9

Note: The table lists the yield strength, Young's modulus, stress at break, elongation at break, and calculated toughness derived from the tensile stress–strain curves measured at 22°C (Figure 8). Data are presented as mean value ± standard deviation.

2-EHA units increasing chain mobility and free volume, allowing for extensive plastic deformation before failure.

The toughness—the energy absorbed before break, calculated from the area under the stress–strain curve [41] further highlights this tunability. Cop 70, with a balanced composition, achieves an optimal synergy between the strength imparted by IBOA and the elasticity provided by 2-EHA, resulting in the highest toughness of 4106.8 MJ/m^3, making it exceptionally damage-tolerant. While Cop 80 is strong but not tough, and Cop 50/Cop 60 are soft and highly extensible, it is the fine-tuned intermediate composition that offers the most robust mechanical performance.

The tunability of mechanical properties through comonomer ratio variation renders this copolymer system highly attractive for applications demanding specific performance profiles. Cop 70 demonstrates superior toughness and balanced properties, showing promise for demanding applications such as impact-resistant protective coatings, durable adhesives, or flexible biomedical device components. Cop 80, with its enhanced rigidity, appears suitable for rigid films or molded parts, while the pronounced elasticity of Cop 50 and Cop 60 positions them as ideal candidates for soft robotics, flexible seals, or elastomeric gels. This broad spectrum of properties—unattainable with the homopolymers alone, as PIBOA is excessively brittle and PEHA too tacky and weak for conventional tensile testing—powerfully demonstrates the necessity of copolymerization. Rather than merely adjusting properties, copolymerization proves essential for creating coherent materials with application-specific mechanical performance from these monomer systems.

4 | Conclusions

This study successfully establishes a straightforward and efficient UV-induced free-radical polymerization route to create a novel class of linear random copolymers based on IBOA and 2-EHA. The key innovation lies in the precise and predictable tunability of these materials' thermo-mechanical properties, achieved simply by varying the comonomer ratio.

A combination of advanced characterization techniques provided unprecedented insight into the copolymer structure. While SEC confirmed the formation of high molar mass polymers, a multi-faceted NMR and MALDI-TOF MS analysis, supported by a custom computational algorithm, definitively confirmed the random microstructure. The formation of a statistical copolymer rather than a mixture of homopolymers is supported by ^{1}H NMR spectra. The spectra lack distinct homopolymer signatures, and MALDI-TOF analysis reveals a single, unimodal copolymer chain distribution. This approach proved exceptionally powerful in deciphering the complex copolymer architecture, including end-group analysis, and can be regarded as a robust methodological framework for characterizing complex copolymer systems.

The most significant finding is the direct correlation between composition and properties. The glass transition temperature (T_g) could be systematically engineered across a wide range (−66°C to 42°C). More importantly, tensile testing demonstrated that this thermal tunability translates directly into a remarkable spectrum of mechanical behavior—from rigid and brittle to soft and highly elastomeric. The identification of an optimal composition (Cop 70) that exhibits exceptional toughness by balancing the rigid IBOA segments with the flexible 2-EHA units is a key outcome.

This work moves beyond simple synthesis to present a versatile material platform. The ability to dial in specific properties by adjusting a single parameter (comonomer ratio) makes these poly(IBOA-co-2EHA) copolymers highly promising candidates for a wide range of applications, from high-performance, impact-resistant coatings and flexible electronics to soft robotics and tailored biomedical devices, where specific and predictable mechanical performance is critical.

Author Contributions

Djazia Bendeddouche: formal analysis (lead), investigation (equal), visualization (equal), writing – original draft (equal). **Lamia Bedjaoui-Alachaher:** funding acquisition (lead), project administration (equal), supervision (lead), writing – review and editing (equal). **Aida Jover:** formal analysis (equal), validation (equal), visualization (equal). **Mohammed Aymen Zehouani:** software (equal), validation (equal). **Amina Bouriche:** formal analysis (equal), validation (equal). **Anne-Sophie Schuller:** methodology (equal), visualization (equal). **Christelle Delaite:** methodology (equal), visualization (equal). **Ulrich Maschke:** conceptualization (equal), methodology (supporting), project administration (equal), writing – review and editing (lead).

Acknowledgments

This work was supported by an international research program. The authors gratefully acknowledge support from the Algerian Ministry

of Higher Education and Scientific Research (MESRS), the General Directorate of Scientific Research and Technological Development (DGRSDT) of Algeria, and the University of Tlemcen. Support from the Spanish Ministry of Science and Innovation (Grant No. PID2023-147148NB-I00), the University of Haute-Alsace Mulhouse (France), and the University of Lille (France) is also sincerely acknowledged.

Conflicts of Interest

The authors declare no conflicts of interest.

Data Availability Statement

The authors have nothing to report.

References

1. N. Ide and T. Fukuda, "Nitroxide-Controlled Free-Radical Copolymerization of Vinyl and Divinyl Monomers. 2. Gelation," *Macromolecules* 32 (1999): 95–99, https://doi.org/10.1021/ma9805349.

2. W. A. Braunecker and K. Matyjaszewski, "Controlled/Living Radical Polymerization: Features, Developments, and Perspectives," *Progress in Polymer Science* 32 (2007): 93–146, https://doi.org/10.1016/j.progpolymsci.2006.11.002.

3. M. Kury, K. Ehrmann, C. Gorsche, et al., "Regulated Acrylate Networks as Tough Photocurable Materials for Additive Manufacturing," *Polymer International* 71 (2022): 897–905, https://doi.org/10.1002/pi.6364.

4. G. M. Russell, T. Kaneko, S. Ishino, H. Masai, and J. Terao, "Transient Photodegradability of Photostable Gel Induced by Simultaneous Treatment With Acid and UV–Light for Phototuning of Optically Functional Materials," *Advanced Functional Materials* 32 (2022): 2205855, https://doi.org/10.1002/adfm.202205855.

5. L. M. Sáiz, M. G. Prolongo, V. Bonache, A. Jiménez-Suárez, and S. G. Prolongo, "Self-Healing Materials Based on Disulfide Bond-Containing Acrylate Networks," *Polymer Testing* 117 (2023): 107832, https://doi.org/10.1016/j.polymertesting.2022.107832.

6. A. Spessa, R. Bongiovanni, and A. Vitale, "A Novel Disulfide-Containing Monomer for Photoinitiator-Free Self-Healable Photocured Coatings," *Progress in Organic Coatings* 187 (2024): 108098, https://doi.org/10.1016/j.porgcoat.2023.108098.

7. Y. Nie, R. Liu, N. Yao, et al., "UV-Curable Castor-Oil-Based Multi-Crosslinking Polymer Networks Containing Dynamic Disulfide Bonds: High Toughness, Self-Healing, and Shape Memory Properties," *Polymer Testing* 118 (2023): 107879, https://doi.org/10.1016/j.polymertesting.2022.107879.

8. X. Chen, Y. Wang, Z. Cheng, J. Wei, Y. Shi, and J. Qian, "Diffusion Behavior of Drug Molecules in Acrylic Pressure-Sensitive Adhesive," *ACS Omega* 5 (2020): 9408–9419, https://doi.org/10.1021/acsomega.0c00491.

9. X. Wang, L. Nan, H. Song, et al., "3-Methacryloxypropyltrimethoxy silane-Modified Hydroxyl Acrylate Pressure-Sensitive Adhesive With High Antiplasticity for Efficient Transdermal Drug Delivery," *ACS Applied Polymer Materials* 6 (2024): 2972, https://doi.org/10.1021/acsapm.3c03208.

10. S. Grauzeliene, A.-S. Schuller, C. Delaite, and J. Ostrauskaite, "Biobased Vitrimer Synthesized From 2-Hydroxy-3-Phenoxypropyl Acrylate, Tetrahydrofurfuryl Methacrylate and Acrylated Epoxidized Soybean Oil for Digital Light Processing 3D Printing," *European Polymer Journal* 198 (2023): 112424, https://doi.org/10.1016/j.eurpolymj.2023.112424.

11. S. Grauzeliene, A.-S. Schuller, C. Delaite, and J. Ostrauskaite, "Development and Digital Light Processing 3D Printing of a Vitrimer Composed of Glycerol 1, 3-Diglycerolate Diacrylate and Tetrahydrofurfuryl Methacrylate," *ACS Applied Polymer Materials* 5 (2023): 6958, https://doi.org/10.1021/acsapm.3c01018.

12. S. Pruksawan, Y. T. Chong, W. Zen, T. J. E. Loh, and F. Wang, "Sustainable Vat Photopolymerization-Based 3D-Printing Through Dynamic Covalent Network Photopolymers," *Chemistry–An Asian Journal* 19 (2024): e202400183, https://doi.org/10.1002/asia.202400183.

13. Q. Ge, A. H. Sakhaei, H. Lee, C. K. Dunn, N. X. Fang, and M. L. Dunn, "Multimaterial 4D Printing With Tailorable Shape Memory Polymers," *Scientific Reports* 6 (2016): 31110, https://doi.org/10.1038/srep31110.

14. T. Abdullah and O. Okay, "4D Printing of Body Temperature-Responsive Hydrogels Based on Poly(Acrylic Acid) With Shape-Memory and Self-Healing Abilities," *ACS Applied Bio Materials* 6 (2023): 703–711, https://doi.org/10.1021/acsabm.2c00939.

15. J. Brandrup, E. H. Immergut, and E. A. Grulke, *Polymer Handbook*, 4th ed. (Wiley, 2003).

16. A. Bouriche, A. Barrera, C. Binet, et al., "From Residual Mesogens to Responsive Materials: Recycled Liquid Crystals From End-of-Life Screens in Photocurable Acrylate Networks," *University Politehnica of Bucharest Scientific Bulletin, Series A: Applied Mathematics and Physics* 87, no. 2 (2025): 209–222.

17. C. Corsaro, G. Neri, A. Santoro, and E. Fazio, "Acrylate and Methacrylate Polymers' Applications: Second Life With Inexpensive and Sustainable Recycling Approaches," *Materials* 15 (2021): 282, https://doi.org/10.3390/ma15010282.

18. G. Moretti, L. Sarina, L. Agostini, R. Vertechy, G. Berselli, and M. Fontana, "Styrenic-Rubber Dielectric Elastomer Actuator With Inherent Stiffness Compensation," *Actuators* 9 (2020): 44, https://doi.org/10.3390/act9020044.

19. D. Merah, L. Bedjaoui, N. Zeggai, et al., "Enhanced Thermal Stability of Biobased Crosslinked Poly (Isobornylacrylate-co-2-Ethylhexylacrylate) Copolymers," *Journal of Polymer Research* 29 (2022): 266, https://doi.org/10.1007/s10965-022-03139-7.

20. N. Zeggai, Z. Bouberka, F. Dubois, et al., "Effect of Structure on the Glass Transition Temperatures of Linear and Crosslinked Poly(Isobornylacrylate-Co-Isobutylacrylate)," *Journal of Applied Polymer Science* 138 (2021): 50449, https://doi.org/10.1002/app.50449.

21. W. Jakubowski, A. Juhari, A. Best, K. Koynov, T. Pakula, and K. Matyjaszewski, "Comparison of Thermomechanical Properties of Statistical, Gradient and Block Copolymers of Isobornyl Acrylate and n-Butyl Acrylate With Various Acrylate Homopolymers," *Polymer* 49 (2008): 1567–1578, https://doi.org/10.1016/j.polymer.2008.01.047.

22. M. M. Alam, K. S. Jack, D. J. Hill, A. K. Whittaker, and H. Peng, "Gradient Copolymers – Preparation, Properties and Practice," *European Polymer Journal* 116 (2019): 394–414, https://doi.org/10.1016/j.eurpolymj.2019.04.028.

23. F. Dong, Y. Qian, X. Xu, et al., "Preparation and Characterization of UV-Curable Waterborne Polyurethane Using Isobornyl Acrylate Modified via Copolymerization," *Polymer Degradation and Stability* 184 (2021): 109474, https://doi.org/10.1016/j.polymdegradstab.2020.109474.

24. D. Khandelwal, S. Hooda, and A. S. Brar, "Configurational Sequence Determination of Poly(Isobornyl Acrylate) by NMR Spectroscopy," *Journal of Molecular Structure* 991 (2011): 24–30, https://doi.org/10.1016/j.molstruc.2011.01.017.

25. D. Khandelwal, S. Hooda, A. S. Brar, and R. Shankar, "1D and 2D NMR Studies of Isobornyl Acrylate—Methyl Methacrylate Copolymers," *Journal of Molecular Structure* 1004 (2011): 121–130, https://doi.org/10.1016/j.molstruc.2011.07.046.

26. D. Khandelwal, S. Hooda, A. S. Brar, and R. Shankar, "Stereoregularity Evolution of Isobornyl Acrylate and Styrene Copolymers by 2D

NMR Spectroscopy," *Journal of Molecular Structure* 1049 (2013): 99–111, https://doi.org/10.1016/j.molstruc.2013.05.046.

27. D. Merah, U. Maschke, N. Bouchikhi, H. Ziani Chérif, and L. Bedjaoui-Alachaher, "Characterization of Swelling Behavior and Elastomer Properties of Acrylate Polymers Containing 2-Ethylhexyl and Isobornyl Esters," *Polymer Bulletin* 80 (2023): 10073, https://doi.org/10.1007/s00289-022-04491-w.

28. N. Zeggai, B. D. Youcef, F. Dubois, et al., "Analysis of Dynamic Mechanical Properties of Photochemically Crosslinked Poly(Isobornylacrylate-Co-Isobutylacrylate) Applying WLF and Havriliak-Negami Models," *Polymer Testing* 72 (2018): 432–438, https://doi.org/10.1016/j.polymertesting.2018.10.038.

29. N. Zeggai, Z. Bouberka, F. Dubois, et al., "Tuning of Thermally-Induced Shape Memory Properties of Low-Cost Biocompatible Linear and Chemically Crosslinked Isobornyl/Isobutylacrylate Copolymers," *Composites Science and Technology* 219 (2022): 109213, https://doi.org/10.1016/j.compscitech.2021.109213.

30. P. B. Bamane and R. N. Jagtap, "Development of a Water-Based Functional Additive by Using Isobornyl Acrylate Copolymer to Improve Ink-Adhesion on Untreated Polypropylene Surfaces: A Comparative Approach," *International Journal of Adhesion and Adhesives* 121 (2023): 103311, https://doi.org/10.1016/j.ijadhadh.2022.103311.

31. A. Benkhelifa, K. E. Boudraa, and T. Bouchaour, "Enhancement of Shape Memory Properties of Thermo-Responsive Copolymers-Based 2-Hydroxy Propyl Methacrylate and n-Isobornyl Acrylate," *Journal of Thermal Analysis and Calorimetry* 147 (2022): 13313–13328, https://doi.org/10.1007/s10973-022-11532-z.

32. H. Xu, F. Qiu, Y. Wang, W. Wu, D. Yang, and Q. Guo, "UV-Curable Waterborne Polyurethane-Acrylate: Preparation, Characterization and Properties," *Progress in Organic Coatings* 73 (2012): 47–53, https://doi.org/10.1016/j.porgcoat.2011.08.019.

33. G. Montaudo and R. P. Lattimer, *Mass Spectrometry of Polymers* (CRC Press, 2001).

34. H. Pasch and W. Schrepp, *MALDI-TOF Mass Spectrometry of Synthetic Polymers* (Springer, 2003).

35. M. S. Montaudo, C. Puglisi, S. Battiato, S. Zappia, S. Destri, and F. Samperi, "An Innovative Approach for the Chemical Structural Characterization of Poly(Styrene 4-Vinylpyridine) Copolymers by Matrix-Assisted Laser Desorption/Ionization Time of Flight Mass Spectrometry," *Journal of Applied Polymer Science* 136 (2019): 46976, https://doi.org/10.1002/app.46976.

36. A. C. Crecelius, C. R. Becer, K. Knop, and U. S. Schubert, "Block Length Determination of the Block Copolymer mPEG-b-PS Using MALDI-TOF MS/MS," *Journal of Polymer Science, Part A: Polymer Chemistry* 48 (2010): 4375, https://doi.org/10.1002/pola.24223.

37. G. Wilczek-Vera, P. O. Danis, and A. Eisenberg, "Individual Block Length Distributions of Block Copolymers of Polystyrene-Block-Poly(α-Methylstyrene) by MALDI/TOF Mass Spectrometry," *Macromolecules* 29 (1996): 4036–4044, https://doi.org/10.1021/ma9516394.

38. S. Hosseini, F. Ibrahim, I. Djordjevic, and L. H. Koole, "Polymethyl Methacrylate-Co-Methacrylic Acid Coatings With Controllable Concentration of Surface Carboxyl Groups: A Novel Approach in Fabrication of Polymeric Platforms for Potential Bio-Diagnostic Devices," *Applied Surface Science* 300 (2014): 43–50, https://doi.org/10.1016/j.apsusc.2014.01.203.

39. R. M. Jones, *Mechanics of Composite Materials*, 2nd ed. (CRC Press, 2018).

40. B. Wang and A. Facchetti, "Mechanically Flexible Conductors for Stretchable and Wearable E-Skin and E-Textile Devices," *Advanced Materials* 31 (2019): 1901408, https://doi.org/10.1002/adma.201901408.

41. I. M. Ward and J. Sweeney, *Mechanical Properties of Solid Polymers*, 3rd ed. (Wiley, 2013).

Supporting Information

Additional supporting information can be found online in the Supporting Information section. **Data S1:** Supporting Information.